# Fine-Tuned Intrinsically Ultramicroporous Polymers Redefine the Permeability/Selectivity Upper Bounds of Membrane-Based Air and Hydrogen Separations

Raja Swaidan, Bader Ghanem, and Ingo Pinnau*

Advanced Membranes and Porous Materials Center (AMPMC), Physical Sciences and Engineering Division, King Abdullah University of Science and Technology (KAUST), Thuwal, 23955-6900, Saudi Arabia

S *Supporting Information*

ABSTRACT: Intrinsically ultramicroporous (<7 Å) polymers represent a new paradigm in materials development for membrane-based gas separation. In particular, they demonstrate that uniting intrachain "rigidity", the traditional design metric of highly permeable polymers of intrinsic microporosity (PIMs), with gas-sieving ultramicroporosity yields high-performance gas separation membranes. Highly ultramicroporous PIMs have redefined the state-of-the-art in large-scale air (e.g., O_2/N_2) and hydrogen recovery (e.g., H_2/N_2, H_2/CH_4) applications with unprecedented molecular sieving gas transport properties. Accordingly, presented herein are new 2015 permeability/selectivity "upper bounds" for large-scale commercial membrane-based air and hydrogen applications that accommodate the substantial performance enhancements of recent PIMs over preceding polymers. A subtle balance between intrachain rigidity and interchain spacing has been achieved in the amorphous microstructures of PIMs, fine-tuned using unique bridged-bicyclic building blocks (i.e., triptycene, ethanoanthracene and Tröger's base) in both ladder and semiladder (e.g., polyimide) structures.

Rigid, contorted macromolecules

Fast molecular sieving *ultra*-microporosity
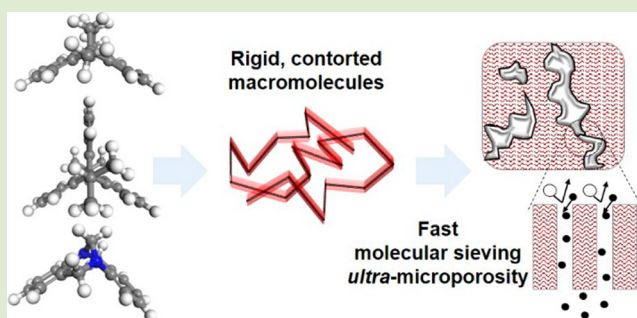
Polymer membrane technology is a simple low-energy intensity alternative to traditional gas separation technologies such as cryogenic distillation and absorption.[1,2] It is well established in various applications, with nearly two-thirds of the market comprising air enrichment (e.g., for nitrogen blanketing or oxygen-enhanced combustion) and hydrogen recovery (e.g., from ammonia purge gas and petrochemical refinery reactor streams).[3,4] Membrane materials performance and, thus, viability are gauged by the polymer permeability and selectivity. In 1991, Robeson[5,6] established that these two intrinsic material properties obey a trade-off relationship for polymers, whereby more permeable materials tend to be less selective and vice versa, and more recently, updated the database in 2008. Accordingly, the state of the art for a given gas pair is traditionally identified by a linear "upper bound" fit to the top performing materials on a log−log plot of available permeability/selectivity combinations. Freeman provided the fundamental theoretical basis of these upper bound gas pair relationships.[7] Highly selective but low-permeability commercially available polymers, such as cellulose acetate, polysulfone, polyimide, and polycarbonate, continue to be industrially employed in air and hydrogen separations since the 1980s, and a key challenge driving research has been to develop new polymers that defy the "upper bound" trade-off relationships and unite high selectivities with high permeabilities.

Polymers of intrinsic microporosity (PIMs) are a rapidly expanding class of solution-processable amorphous glassy polymers designed for membrane separations. Traditionally, PIMs integrate microporosity (<20 Å) by virtue of rigid and contorted macromolecular architectures that pack inefficiently in the solid state.[8−25] The earliest PIMs were principally based on such "rigid" design metrics and included substituted polyacetylenes. For example, poly(1-trimethylsilyl-1-propyne) [PTMSP] was characterized by very high free volume (∼30%), a high BET surface area of ∼900 m^2 g^{-1}, and gas diffusion coefficients 3−6 orders of magnitude higher than those of any known preceding polymers. Because of its large average interchain pore size, PTMSP still exhibits among the highest reported gas permeabilities, which are, however, coupled with the lowest gas selectivities, making it an unattractive membrane material for air and hydrogen separations.[26]

Importantly, polymer structure/property optimizations have recently revealed that exceptional molecular sieving transport, characterized by balanced combinations of permeability and selectivity, is attainable by a unique class of PIMs that augment the traditional focus on intrachain "rigidity", with an emphasis on interchain spacing in the gas-sieving ultramicroporous domain. That is, ultramicroporous PIMs have demonstrated that when bridged-bicyclic contortion centers (Figure 1a) are integrated into a "rigid," predominantly fused-ring, backbones
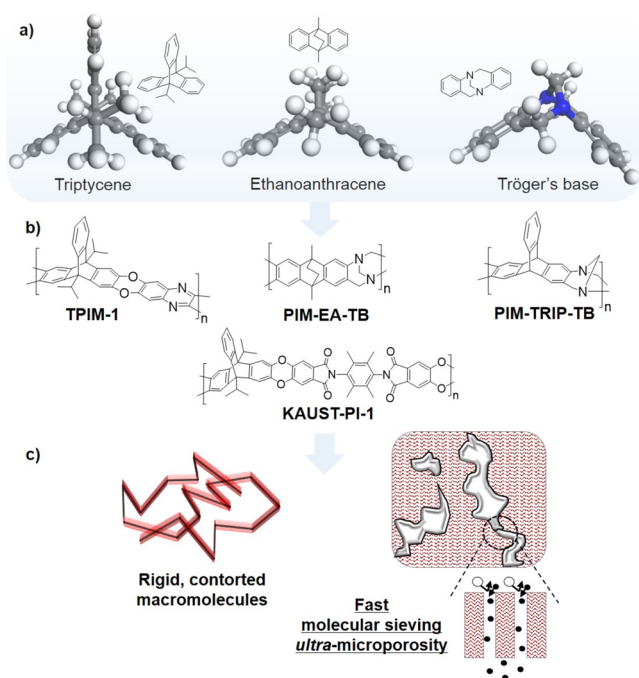
Figure 1. (a) Three core bridged-bicyclic building blocks for intrinsically ultramicroporous PIMs. (b) Representative ladder and semiladder PIMs recently derived from those building blocks that have redefined the state-of-the-art in membrane-based air and hydrogen separations. (c) Schematic illustrating how rigid and contorted PIMs are envisioned to produce an amorphous microstructure containing large, permeable "pores" linked with smaller, ultramicropores (<7 Å) to facilitate high permeability with high selectivity.

results in exemplary ladder PIMs[17,19,23] and semiladder PIM-polyimides (PIM−PIs;[18,22,24,27,28] Figure 1b), bridging the gap between high permeability and high selectivity for unprecedented performance in high-impact, energy-demanding air and hydrogen separations. Figure 1a illustrates the three most promising core building blocks currently employed in the design of highly ultramicroporous PIMs, namely, 9,10-diisopropyl-triptycene, dimethyl-ethanoanthracene, and Tröger's base and highlights their nearly identical ~120° kinks. Indeed, the geometry of the contortion site has been increasingly emphasized given the inferior performances observed for analogous polymers containing traditional 90°-

oriented spirobisindane-based contortion sites (e.g., in prototypical PIM-1 and PIM-7).[18,19,22] Similar improvements in molecular sieving behavior of PIM-1 have been achieved using controlled thermal-oxidative cross-linking at 350−400 °C (TOX-PIM-1),[29] but such thermally treated films (including thermally rearranged and carbon films) have not traditionally been considered in construction of the upper bounds to polymer membrane-based gas separation.

In general, relative to the microstructures of conventional low-free-volume polymers, a unique attribute of rigid, glassy PIM microstructures is a distribution of interconnected "porosity" that is permanent on the time-scale of gas permeation.[30] Therefore, in conventional polymers, gas transport occurs via slow, thermally activated diffusion through transient chain openings. In PIMs, open "pores" derived from inefficient packing of rigid and contorted chains readily permit fast gas diffusion and, thus, higher permeability. A major advantage of the PIMs in Figure 1b, reported by the groups of McKeown et al. and Pinnau et al., is they simultaneously offer high selectivity owing to an interconnected porosity in the ultramicroporous (<7 Å) domain critical to gas separation. Figure 1c illustrates how such molecular-sieving behavior may be realized in PIMs, where larger, highly permeable pores are envisioned to be interconnected with smaller, selective ultramicropores. That is, the highly ultramicroporous PIMs of Figure 1b feature a subtle balance between intrachain rigidity and interchain spacing,[22] which has been long believed to be essential to realizing new heights in separation performance.[7,31]

Figure 2a concisely presents key results from physisorption-based assessments of amorphous polymer microstructures that support the above discussion: (i) Large gas uptake at low pressures indicated high microporosity in rigid PIMs, including PTMSP, PIM-1, and TPIM-1, whereas little was observed in efficiently packing low-free-volume polymers like poly-(phenylene oxide) [PPO];[32] (ii) high free volumes were qualitatively indicated for the PIMs by nearly 2 orders of magnitude higher BET surface areas than for PPO; and (iii) more uptake in the ultra-low-pressure region (Figure 2a, inset) for triptycene-based TPIM-1 indicated the presence of a narrower microporosity than for spiro-based PIM-1, with PTMSP showing the lowest uptake and, therefore, the largest micropores. Pore-size distributions derived via an NLDFT analysis of the isotherms (Figure 2b) qualitatively indicated a shift into the ultramicroporous domain for the highly
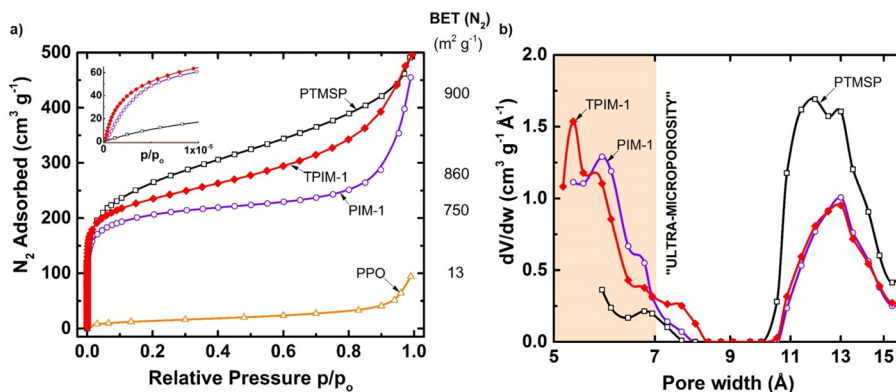
Figure 2. (a) Nitrogen adsorption isotherms (77 K) by PIMs, including PTMSP, TPIM-1, and PIM-1, and for conventional low-free-volume poly(phenylene oxide) [PPO]. The BET surface areas are listed beside the right axis. (b) NLDFT-derived pore-size distribution analyses on the isotherms, assuming carbon slit pores.

permeable and selective TPIM-1, which is in contrast to a dominant contribution of larger pores to the microstructure in the highly permeable but poorly selective PTMSP.

The outstanding O_2/N_2 separation properties for homogeneous and isotropic films of notable PIMs reported to date are presented in Figure 3. The resulting scatter reaches significantly
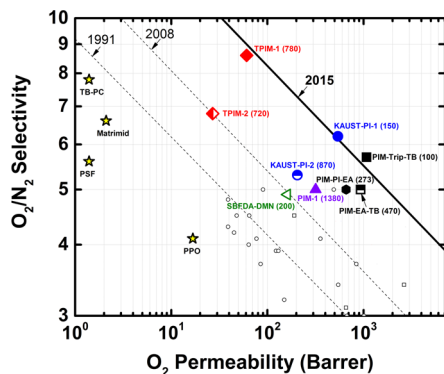
Figure 3. 2015 "upper bound" to polymer membrane performance in O_2/N_2 separation, defined by outstanding PIMs. Previous 1991 and 2008 upper bounds (dashed lines) are included to evidence the substantial shift in the state-of-the-art. The "age" of the polymer in days after methanol treatment is indicated in parentheses. The yellow stars indicate commercially used membrane materials. The small open circles and squares represent other semiladder PIM-polyimides[22,37,38] and ladder PIMs.[19,20,39]

beyond the latest 2008 Robeson upper bound and, thus, warrants introduction of a new upper bound that defines a new state of the art.[6] Interestingly, a visual fit to the best performing PIMs (i.e., Figure 1b) yields a linear line over nearly two decades of permeability (i.e., via equation $P_i = k\alpha_{ij}^n$, where k is a front factor and n is the slope) with a slope practically identical to that reported in 1991 and 2008.[5,6] This is consistent with Freeman's theoretical prediction that the slope of the upper bound should be fixed for a given gas pair (i.e., slope $\alpha \ (d_j/d_i)^2$, where d_i may be the kinetic diameter of component i).[7,33,34] Also, in line with Freeman's theory, a large increase in the front factor, k, which is a function of gas solubility,[7] is expected since the high free volume in the PIMs defining the new line considerably boosts sorption capacity (e.g., Figure 2).[35] Furthermore, the shift from the 2008 line to the 2015 line is much greater than that between the 1991 and 2008 lines, illustrating the substantial impact of molecular sieving PIMs. The discussion for the hydrogen separations is analogous and new 2015 H_2/N_2 and H_2/CH_4 upper bounds are shown in Figure 4a,b. Parameters for the new 2015 upper bounds are provided in Table 1. For validation, the permeabilities and selectivities of the PIMs near to or defining the 2015 upper bounds are listed in Table 2.

An important point must be made regarding film preparation and the determination of gas transport properties in PIMs, which is relevant to the positioning of the new 2015 upper bounds. Upon slow evaporative casting, the films were all soaked in a nonsolvent (e.g., methanol) to exchange residual casting solvent trapped in the micropores. Because the soak imparts significant excess nonequilibrium free volume to the films, freshly measured permeability and selectivity data taken are transient-state data and not meaningful to be placed on upper bounds. Therefore, sufficient time must be allowed for (i) the structures to relax into a "quasi-equilibrium" state and
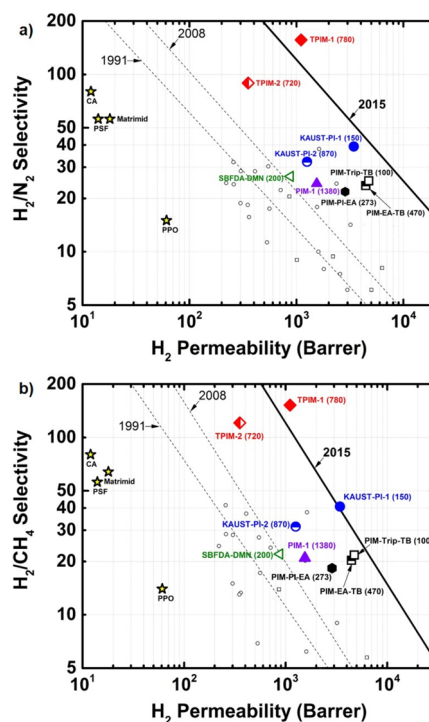
Figure 4. 2015 "upper bound" to polymer membrane performance in (a) H_2/N_2 and (b) H_2/CH_4 separations defined by outstanding PIMs. Previous 1991 and 2008 upper bounds (dashed lines) are included to evidence the substantial shift in the state-of-the-art. The "age" of the polymer in days after methanol treatment is indicated in parentheses. The yellow stars indicate commercially used membrane materials. The small open circles and squares represent other semiladder PIM-polyimides[22,37,38] and ladder PIMs.[19,20,39]

(ii) for consistent measurement of the intrinsic permeation properties of the films to be reported.[22,24,36] That is, reporting PIM transport data just after methanol treatment is inappropriate given that the physically aging polymer structure is in a dynamic state. Figures S1, S2, and S3 (Supporting Information) illustrate the evolution of KAUST-PI-1, TPIM-1, TPIM-2, PIM-1, SBFDA-DMN PIM-EA-TB, and PIM-Trip-TB gas transport properties in days after methanol treatment for the various gas pairs. Importantly, beyond two weeks, the trajectories begin to parallel the presented 2015 upper bounds, thereby further validating their positioning with the given data. This observation withstanding, the "ages" of the samples used to construct the upper bounds are provided in parentheses next to the labels in Figures 3 and 4.

In conclusion, the new 2015 permeability/selectivity upper bound lines presented herein reflect the substantial progress PIMs contribute to the state of the art in membrane-based air and hydrogen separations. The combination of rigidity and ultramicroporosity, which is fine-tuned via the use of bridged-bicyclic building blocks, allows the resulting polymers to bridge the gap between the high permeabilities of standard PIMs and the high selectivities of low-free-volume commercial-type materials. Importantly, the resulting PIMs defy trade-off relationships in matching the practical selectivities of commercial materials with desired orders-of-magnitude higher permeabilities. The resulting performance represents a major step forward in material development and offers great potential to expand the industrial horizons of polymer membrane-based gas separation technology.

Table 1. Overview of "Upper Bound" Line Parameters, where $P_i = k\alpha_{ij}^n$ (i.e., P_i is Permeability of i in Barrer, k is the Front Factor in Barrer, α_{ij} is the Selectivity for i/j, and n is the Slope), for Key Polymer Membrane-Based Air and Hydrogen Separations

	1991		2008		2015	
gas pair	k (Barrer)	N	k (Barrer)	n	k (Barrer)	n
O_2/N_2	3.89×10^5	-5.800	1.40×10^6	-5.666	1.67×10^7	-5.70
H_2/N_2	5.29×10^4	-1.5275	9.77×10^4	-1.484	1.10×10^6	-1.46
H_2/CH_4	1.85×10^4	-1.2112	2.72×10^4	-1.107	1.95×10^5	-1.10

Table 2. Performance of PIMs near to or Defining the New 2015 Upper Bounds for Key Polymer Membrane-Based Air (e.g., O_2/N_2) and Hydrogen (e.g., H_2/N_2, H_2/CH_4) Separations

	air		hydrogen		
polymer	O_2 permeability (Barrer)	O_2/N_2 selectivity	H_2 permeability (Barrer)	H_2/N_2 selectivity	H_2/CH_4 selectivity
TPIM-1	61	8.6	1105	156	152
KAUST-PI-1	542	6.2	3431	39	41
PIM-TRIP-TB	1073	5.7	4740	25	22
PIM-EA-TB	933	5.0	4442	24	20

■ ASSOCIATED CONTENT

Ⓢ Supporting Information

The evolution of gas transport properties over time for methanol-treated PIMs is provided on permeability/selectivity maps for O_2/N_2, H_2/N_2, and H_2/CH_4 separations. The Supporting Information is available free of charge on the ACS Publications website at DOI: 10.1021/acsmacrolett.5b00512.

(PDF)

■ AUTHOR INFORMATION

Corresponding Author
*Tel.: +966-12-808-2406. E-mail: ingo.pinnau@kaust.edu.sa.

Notes
The authors declare no competing financial interest.

■ ACKNOWLEDGMENTS

■ REFERENCES

(1) Sanders, D. E.; Smith, Z. P.; Guo, R. L.; Robeson, L. M.; McGrath, J. E.; Paul, D. R.; Freeman, B. D. *Polymer* **2013**, *54*, 4729−4761.
(2) Oak Ridge National Laboratory. *Materials Research for Separations Technologies: Energy and Emission Reduction Opportunities*; U.S. Dept. of Energy: Washington, DC, 2005; http://www1.eere.energy.gov/manufacturing/industries_technologies/imf/pdfs/separationsreport.pdf.
(3) Baker, R. W. *Ind. Eng. Chem. Res.* **2002**, *41*, 1393−1411.
(4) Baker, R. W.; Low, B. T. *Macromolecules* **2014**, *47*, 6999−7013.
(5) Robeson, L. M. *J. Membr. Sci.* **1991**, *62*, 165−185.
(6) Robeson, L. M. *J. Membr. Sci.* **2008**, *320*, 390−400.
(7) Freeman, B. D. *Macromolecules* **1999**, *32*, 375−380.
(8) McKeown, N. B. *ISRN Materials Science* **2012**, *2012*, 16.
(9) Budd, P. M.; Ghanem, B. S.; Makhseed, S.; McKeown, N. B.; Msayib, K. J.; Tattershall, C. E. *Chem. Commun.* **2004**, 230−231.
(10) Budd, P. M.; McKeown, N. B.; Fritsch, D. *J. Mater. Chem.* **2005**, *15*, 1977−1986.
(11) Budd, P. M.; Msayib, K. J.; Tattershall, C. E.; Ghanem, B. S.; Reynolds, K. J.; McKeown, N. B.; Fritsch, D. *J. Membr. Sci.* **2005**, *251*, 263−269.
(12) Budd, P. M.; McKeown, N. B.; Ghanem, B. S.; Msayib, K. J.; Fritsch, D.; Starannikova, L.; Belov, N.; Sanfirova, O.; Yampolskii, Y.; Shantarovich, V. *J. Membr. Sci.* **2008**, *325*, 851−860.
(13) Maier, G. *Angew. Chem., Int. Ed.* **2013**, *52*, 4982−4984.
(14) Guiver, M. D.; Lee, Y. M. *Science* **2013**, *339*, 284−285.
(15) Du, N. Y.; Park, H. B.; Robertson, G. P.; Dal-Cin, M. M.; Visser, T.; Scoles, L.; Guiver, M. D. *Nat. Mater.* **2011**, *10*, 372−375.
(16) Thomas, S.; Pinnau, I.; Du, N. Y.; Guiver, M. D. *J. Membr. Sci.* **2009**, *333*, 125−131.
(17) Carta, M.; Croad, M.; Malpass-Evans, R.; Jansen, J. C.; Bernardo, P.; Clarizia, G.; Friess, K.; Lanč, M.; McKeown, N. B. *Adv. Mater.* **2014**, *26*, 3526−3531.
(18) Rogan, Y.; Malpass-Evans, R.; Carta, M.; Lee, M.; Jansen, J. C.; Bernardo, P.; Clarizia, G.; Tocci, E.; Friess, K.; Lanc, M.; McKeown, N. B. *J. Mater. Chem. A* **2014**, *2*, 4874−4877.
(19) Carta, M.; Malpass-Evans, R.; Croad, M.; Rogan, Y.; Jansen, J. C.; Bernardo, P.; Bazzarelli, F.; McKeown, N. B. *Science* **2013**, *339*, 303−307.
(20) Bezzu, C. G.; Carta, M.; Tonkins, A.; Jansen, J. C.; Bernardo, P.; Bazzarelli, F.; McKeown, N. B. *Adv. Mater.* **2012**, *24*, 5930−5933.
(21) Ghanem, B. S.; McKeown, N. B.; Budd, P. M.; Selbie, J. D.; Fritsch, D. *Adv. Mater.* **2008**, *20*, 2766−2771.
(22) Swaidan, R.; Al-Saeedi, M.; Ghanem, B.; Litwiller, E.; Pinnau, I. *Macromolecules* **2014**, *47*, 5104−5114.
(23) Ghanem, B. S.; Swaidan, R.; Ma, X.; Litwiller, E.; Pinnau, I. *Adv. Mater.* **2014**, *26*, 6696−6700.
(24) Ghanem, B. S.; Swaidan, R.; Litwiller, E.; Pinnau, I. *Adv. Mater.* **2014**, *26*, 3688−3692.
(25) Ma, X. H.; Swaidan, R.; Belmabkhout, Y.; Zhu, Y. H.; Litwiller, E.; Jouiad, M.; Pinnau, I.; Han, Y. *Macromolecules* **2012**, *45*, 3841−3849.
(26) Masuda, T.; Isobe, E.; Higashimura, T.; Takada, K. *J. Am. Chem. Soc.* **1983**, *105*, 7473−7474.
(27) Zhuang, Y. B.; Seong, J. G.; Do, Y. S.; Jo, H. J.; Cui, Z.; Lee, J.; Lee, Y. M.; Guiver, M. D. *Macromolecules* **2014**, *47*, 3254−3262.
(28) Wang, Z.; Wang, D.; Jin, J. *Macromolecules* **2014**, *47*, 7477−7483.
(29) Song, Q. L.; Cao, S.; Pritchard, R. H.; Ghalei, B.; Al-Muhtaseb, S. A.; Terentjev, E. M.; Cheetham, A. K.; Sivaniah, E. *Nat. Commun.* **2014**, *5*, 4813.
(30) Wijmans, J. G.; Baker, R. W. *J. Membr. Sci.* **1995**, *107*, 1−21.
(31) Kim, T. H.; Koros, W. J.; Husk, G. R.; O'Brien, K. C. *J. Membr. Sci.* **1988**, *37*, 45−62.
(32) Ilinitch, O. M.; Fenelonov, V. B.; Lapkin, A. A.; Okkel, L. G.; Terskikh, V. V.; Zamaraev, K. I. *Microporous Mesoporous Mater.* **1999**, *31*, 97−110.

(33) Robeson, L. M.; Smith, Z. P.; Freeman, B. D.; Paul, D. R. *J. Membr. Sci.* **2014**, *453*, 71−83.

(34) Robeson, L. M.; Freeman, B. D.; Paul, D. R.; Rowe, B. W. *J. Membr. Sci.* **2009**, *341*, 178−185.

(35) Robeson, L. M.; Liu, Q.; Freeman, B. D.; Paul, D. R. *J. Membr. Sci.* **2015**, *476*, 421−431.

(36) Hill, A. J.; Pas, S. J.; Bastow, T. J.; Burgar, M. I.; Nagai, K.; Toy, L. G.; Freeman, B. D. *J. Membr. Sci.* **2004**, *243*, 37−44.

(37) Ghanem, B. S.; McKeown, N. B.; Budd, P. M.; Al-Harbi, N. M.; Fritsch, D.; Heinrich, K.; Starannikova, L.; Tokarev, A.; Yampolskii, Y. *Macromolecules* **2009**, *42*, 7881−7888.

(38) Rogan, Y.; Starannikova, L.; Ryzhikh, V.; Yampolskii, Y.; Bernardo, P.; Bazzarelli, F.; Jansen, J. C.; McKeown, N. B. *Polym. Chem.* **2013**, *4*, 3813−3820.

(39) Ghanem, B. S.; McKeown, N. B.; Budd, P. M.; Fritsch, D. *Macromolecules* **2008**, *41*, 1640−1646.